THE JOURNAL OF PHYSICAL CHEMISTRY C

Article

pubs.acs.org/JPCC

Carbon Tetrachloride Cold Plasma for Extensive Chlorination of Carbon Nanotubes

Víctor K. Abdelkader,[†] Simone Scelfo,[†] Celeste García-Gallarín,[‡] M. Luz Godino-Salido,[‡] María Domingo-García,[†] F. Javier López-Garzón,[†] and Manuel Pérez-Mendoza*,[†]

[†]Departamento de Química Inorgánica, Facultad de Ciencias, Universidad de Granada, 18071 Granada, Spain

[‡]Departamento de Química Inorgánica y Orgánica, Facultad de Ciencias Experimentales, Universidad de Jaén, 23071 Jaén, Spain

Supporting Information

ABSTRACT: This article reports a new way to covalently bond chlorine to multiwalled carbon nanotubes (MWCNTs) by using a carbon tetrachloride cold plasma treatment. Several factors controlling the efficiency of the plasma treatment were considered. In particular, the methodology to produce the plasma and the temperature and time of treatment were taken into account. The largest chlorine surface concentration was obtained when the MWCNTs were treated with helium plasma before the CCl_4 plasma to activate the surface. Short periods of plasma treatment (5−10 min) were then sufficient to reach high degrees of chlorination (up to 19.2% by weight) much larger than those previously reported. The functionalization takes place mainly in the borders and defects of the tubes, thus preserving the conjugation existing in the graphene layers. Moreover, the treatments show no influence on the textural characteristics of the nanotubes (i.e., porosity and interlayer spacing). Therefore, the method proposed in this work is an excellent approach to introducing surface chlorine atoms, capable of acting as leaving groups, as a first step for further functionalization with more complex molecules, while preserving the morphology and mechanical properties of the nanotubes still intact.

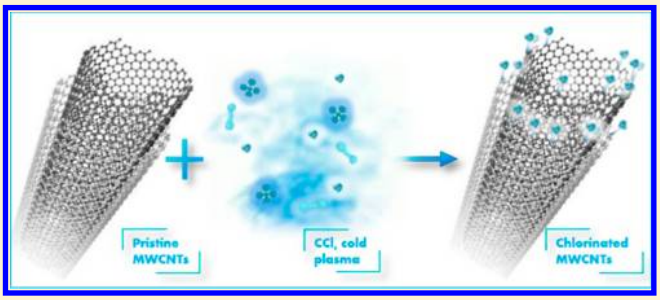

INTRODUCTION

Together with their outstanding mechanical properties, the chemical stability of carbon nanotubes is one of the key factors that have made these materials suitable for a wide range of applications and can be considered as one of their major advantages in many cases. This stability becomes a drawback, however, in attempts to achieve selective and homogeneous functionalization using the common methods employed for other carbon materials. Nevertheless, the functionalization of carbon nanotubes is of high interest, as it widens the field of application of these materials, and effective methods for selectively introducing different surface heteroatoms and complex functions are still being pursued. For instance, the insolubility of carbon nanotubes limits the possibility of obtaining homogeneous dispersions in chemical reactions that need to take place in the solution phase. For this reason, significant efforts have been made to partially dissolve nanotubes in different liquids.[1] Similarly, homogeneous dispersions of nanotubes in carbon nanotube/polymer composites[1−7] have been achieved with carbon nanotubes that were previously functionalized.

Two aspects, among others, are relevant in the functionalization of carbon nanotubes: the sites where the heteroatoms are attached and the degree of functionalization. In relation to the former, the heteroatoms can be attached to caps or open ends of the nanotubes, or they can be bound to the wall atoms. Moreover, carbon nanotubes usually contain irregularities, defects (such as Thrower−Stone−Wales defects), or vacancies,[1,2,8] which have relatively high reactivities, so these are frequently the sites where the heteroatoms are covalently bound. The degree of functionalization is directly related to the reaction conditions, that is, the reactants, their concentrations, and the pressure and temperature. To achieve functionalization with complex molecules, the methodology frequently involves two (or more) stages: a first stage (primary functionalization) dealing with the attachment of heteroatoms such as oxygen, nitrogen, or fluorine,[9,10] among others, and a second stage that uses these heteroatoms as intermediates for further functionalization (secondary functionalization).[1−3,5,11−14] The first step can be crucial, as it opens the possibility of selectively introducing more complex functions onto the surface of the carbon nanotubes.

Primary functionalization with oxygen groups is usually carried out using several oxidants in both the liquid and gas phases, and it results in a large number and variety of oxygen-containing groups such as carboxyl, carbonyl, phenol, and ether groups.[5,15−25] Because of the chemical nature of these groups, only some of them are suitable for secondary functionalization.

Received: May 3, 2013
Revised: July 17, 2013

   dx.doi.org/10.1021/jp404390h | J. Phys. Chem. C XXXX, XXX, XXX−XXX

This suggests that a more selective primary functionalization resulting in only the targeted group(s), able to act as intermediates in the subsequent functionalization steps, could be very useful. For this purpose, fluorine is frequently used for primary functionalization and attachment to carbon nanotube surfaces.[12,26−29] This is not a very difficult task from a thermodynamic point of view because of the high reactivity of fluorine. Nevertheless, the substitution of flouorine for further functionalization once it has been attached to the carbon atoms is not very favored because of the stability of the C—F bond. For this reason, it is desirable to achieve the covalent attachment of another halogen, such as chlorine or bromine, which are much better leaving groups.[30,31] A common procedure for the covalent bonding of chlorine to carbon nanotubes consists of treatment with chlorine gas at relatively high temperature, although other methods have also been reported.[12,32−39]

Based on these facts, the aim of this work was to study new ways to covalently bond chlorine to multiwalled carbon nanotubes (MWCNTs), as chlorine atoms can act as leaving groups in many organic reactions. This makes them a good starting point for obtaining more complex functionalizations. For this purpose, MWCNTs were subjected to microwave cold plasma of carbon tetrachloride. To the best of our knowledge, the use of CCl_4 plasma to functionalize carbon materials has not yet been reported. The advantage of using this procedure for chlorination stems from its simplicity, as it is carried out at low temperature and avoids the use of corrosive gases such as chlorine. Several parameters influencing the degree of MWCNT chlorination and the effect on the characteristics of these carbon materials were investigated in this work.

EXPERIMENTAL SECTION

Commercially available Nanocyl-3100 multiwalled carbon nanotubes (MWCNTs) were used to study functionalization by plasma treatments. The product had an average diameter of 9.5 nm, an average length of 1.5 μm, and 0.6% ash content. These tubes were obtained by the catalytic carbon vapor deposition (CCVD) process. A Europlasma NV device (Junior PLC Advanced SP) was used to generate the plasma. This plasma generator consists of six main parts, namely, vacuum chamber, vacuum pump, high-frequency generator, power distribution rack, and measuring devices. The equipment allows the power, temperature, gas flow, and pressure in the chamber to be controlled. In addition, it allows for the production of plasmas of pure gases and gas mixtures. Carbon tetrachloride (Sigma-Aldrich) was used as the precursor for plasma of chlorine. Several experiments were carried out to optimize the conditions for the attachment of chlorine on the MWCNTs. In particular, carbon tetrachloride was flowed into the plasma chamber in two different forms: as a CCl_4/He mixture and as pure CCl_4. Moreover, the influence of helium plasma pretreatment (for the activation/cleaning of the surface) on the degree of functionalization by both CCl_4/He and pure CCl_4 plasmas was analyzed. In the experiments, 0.5 g of MWCNTs was placed in the plasma chamber and outgassed to a residual pressure of 5 mTorr. Then, the CCl_4/He mixture or pure CCl_4 was admitted to a pressure of 300 or 150 mTorr, respectively, and the system was equilibrated for 3 min. After that, the plasma was produced by the microwave source (2.45 GHz, 300 W). Several periods of plasma treatment, between 0.5 and 45 min, were used. In the case of He plasma pretreatments, once the residual pressure of the chamber reached 5 mTorr, helium was flowed through the chamber up to a pressure of 300 mTorr for 3 min. After that, He plasma was generated by setting up the microwave source to 300 W for 5 min. Then, the chamber was again evacuated to less than 5 mTorr, and the gas reaction mixture (CCl_4/He or pure CCl_4) was admitted without exposing the sample to the air, following the subsequent plasma treatment as described earlier.

The samples were characterized by thermogravimetric analysis (TGA), X-ray photoelectron spectroscopy (XPS), temperature-programmed desorption (TPD), and X-ray diffraction. The TGA measurements were carried out in a Shimadzu TGA-504 device in which the samples were heat-treated in flowing nitrogen (50 mL min^{-1}) at 10 K min^{-1} up to 950 °C. The surface chemical composition of the samples was analyzed by XPS using a Kratos Axis Ultra DLD spectrometer. Monochromatic Al/Mg Kα radiation from a twin anode, in constant-analyzer-energy mode with pass energies of 160 and 20 eV, was used for the survey and high-resolution spectra, respectively. The binding energies were determined by setting up the C 1s transition at 284.6 eV. The high-resolution spectra were fitted to a combination of Lorentzian and Gaussian curves, after background correction, using CasaXPS software, version 2.3.16, Prerel 1.4. TPD profiles were recorded by heating the samples at 10 K min^{-1} in a helium flow (50 mL min^{-1}). The mass evolutions were analyzed in a Pfeiffer Vacuum Omnistar/ThermoStar GSD 320 C mass spectrometer equipped with a quadrupole detector. The X-ray diffractograms were recorded using a Bruker D2 PHASER equipment. The textural characteristics (surface area and porosity) were determined by analyzing the nitrogen adsorption isotherms, which were obtained in an ASAP 2020 apparatus (Micromeritics).

RESULTS AND DISCUSSION

As commented in the Experimental Section, three different methodologies were used for the plasma treatments: (I) a CCl_4/He mixture plasma with previous He plasma pretreatment, (ii) pure CCl_4 plasma with no pretreatment, and (iii) pure CCl_4 plasma with previous He plasma pretreatment. These treatments were each carried out at 30, 40, and 50 °C. The XPS survey spectra of Figure 1 can serve as a summary of the chlorination degrees reached by the three types of treatment. This technique is very useful for analyzing covalent attachment on carbon nanotubes, although solid-state nuclear magnetic resonance (NMR) spectroscopy has also shown direct evidence of covalent functionalization. Thus, the covalent

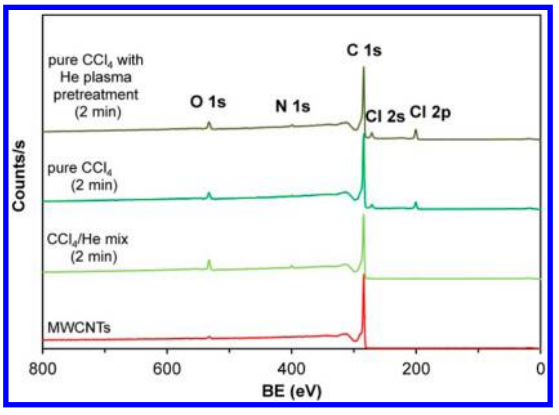

Figure 1. XPS survey spectra of pristine MWCNTs and samples obtained by three different treatments.

dx.doi.org/10.1021/jp404390h | J. Phys. Chem. C XXXX, XXX, XXX−XXX

binding of fluorine to single-walled carbon nanotubes has been characterized by ^{13}C magic-angle-spinning (MAS) NMR spectroscopy. Interestingly, the results obtained by this technique have been correlated to the data obtained by XPS, FTIR, and Raman spectroscopies. Moreover, ^{13}C MAS NMR spectroscopy has also been used to study carboxylic acid-functionalized carbon nanotubes obtained from the previously prepared fluorinated tubes.[9,10] It can be seen that almost no chlorination was produced by the CCl_4/He mixture plasma treatment after 2 min. In fact, the atomic chlorine concentration measured from the XPS spectrum for that sample was 0.1%. The spectrum of the sample obtained by treatment with plasma of pure CCl_4 clearly shows chlorine peaks, which results in a much larger atomic concentration, 4.0%. The different results of the two treatments point to the importance of the higher number of chlorine species in the plasma of pure CCl_4, even though the treatment was carried out at lower pressure. Nevertheless, the intensities of the chlorine peaks of the sample obtained after He plasma pretreatment followed by plasma treatment with pure CCl_4 were even higher, resulting in a chlorine atomic concentration of 5.5%. This is because the helium plasma pretreatment produces carbon free-radical species on the nanotubes (more reactive than normal carbon atoms), which favor further chlorination. Thus, from these data, it is evident that the most efficient of the three procedures, in terms of the amount of chlorine covalently bound to the carbon surface, is the third (He plasma pretreatment + pure CCl_4 plasma). For this reason, this last procedure was chosen for further analysis of the effects of the rest of the variables on the chlorination of the nanotubes.

The XPS survey spectra of some selected samples treated as described previously (Figure 2) clearly show chlorine peaks (Cl 2s and 2p). In addition, these spectra also show an increase of the oxygen O 1s peak (this peak is also in the spectrum of the original MWCNTs) and the presence of the nitrogen N 1s peak. Thus, in some way, the plasma treatment attaches not only chlorine but also oxygen and nitrogen. This might be due to residual air in the plasma chamber, as the final pressure before production of the plasma was 5 mTorr (cf. Experimental Section). In the case of oxygen, it might also be due to postplasma oxygen binding, favored by residual carbon radicals on the surface, when the sample is exposed to atmospheric air and moisture. The appearance of bonded nitrogen after oxygen plasma treatments and an increase in the amount of oxygen after inert gas plasma have been reported.[28,40−49] Moreover, a systematic increase in oxygen when heteroatoms more electronegative than carbon are attached has also been reported.[27,28,32,37] Some authors explained this behavior as a chemisorption process, which is favored by more electronegative heteroatoms.[27] It could be possible that the presence of oxygen and nitrogen is due to air leaking into the plasma system. Nevertheless, the plasma device performed a leak test before every run, so this possibility can be discarded.

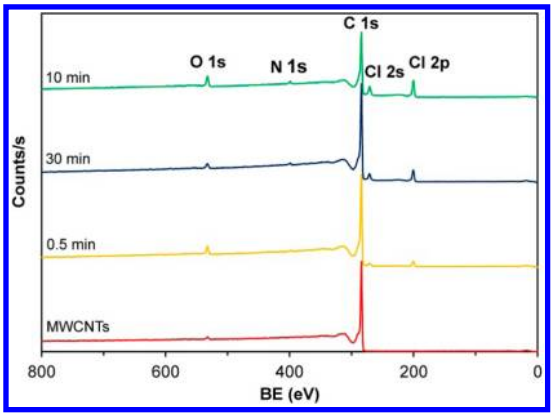

Figure 2. XPS survey spectra of pristine MWCNTs and samples obtained after three different exposure times to pure CCl_4 plasma (with He plasma pretreatment).

We used the XPS survey spectra to determine the heteroatom concentrations. The values, expressed as mass surface concentrations, are collected in Table 1, which also contains the weight losses as obtained from TGA measurements. The weight loss from TGA in the original MWCNTs was larger than the oxygen surface concentration (the only heteroatom in the original sample, cf. Figure 2) as determined by XPS, because of the evolution of groups such as CO and CO_2 during the thermal treatment. Moreover, it is worth mentioning that XPS "sees" only the external surface (only a few nanometers in depth, i.e., several external graphene layers), whereas the TGA measurements refer to the bulk. In contrast to the original nanotubes, the samples obtained after plasma treatments had larger amounts of heteroatoms (i.e., the sum of the weights of chlorine, nitrogen, and oxygen) as determined by XPS than the weight losses obtained by TGA. The comparison of these values with those of the original MWCNTs shows that, when the time of treatment increased, the TGA weight loss exhibited a smaller increase than the total XPS mass concentration. This suggests that the plasma treatments mainly affect the external surface of the nanotubes, which is favored because cold plasmas consist of very reactive species (ions, radicals, electrons, atoms, and neutral species) with low activation energies for surface reaction.[50] As a consequence, the heteroatoms are mainly bound on the external surface of the carbon materials.[51,52]

Table 1. Mass Surface Composition and Weight Loss of Pristine MWCNTs and Samples Obtained after Different Exposure Times

	mass concentration (%)				
sample	O[a]	Cl[a]	N[a]	total[a]	weight loss[b] (%)
MWCNTs	1.39	0.00	0.00	1.39	7.8
0.5 min	4.71	9.01	0.38	14.10	11.1
2 min	4.50	14.47	1.12	20.09	11.3
5 min	4.83	17.91	1.06	23.80	10.9
10 min	6.11	21.37	1.25	28.73	12.0
30 min	3.01	18.31	1.06	22.38	13.0
45 min	3.65	11.74	0.77	16.16	12.8

[a]Values obtained by XPS analysis. [b]Values obtained by TGA.

The influence of the time of plasma treatment in the degree of functionalization is shown in Figure 3, where the atomic concentrations of chlorine are plotted. It is worth mentioning that a significant degree of functionalization (7.6% atomic concentration, i.e., 19.2% by weight) was achieved in only 10 min of treatment. Even at 5 min, the degree of covalent functionalization with chlorine was significant (7.0% atomic concentration, 17.7% by weight), and the surface atomic concentration increased with the time up to 10 min. Longer treatments decreased the atomic concentrations, which is probably due to the competition between the functionalization and the partial etching of carbon atoms at these longer

dx.doi.org/10.1021/jp404390h | J. Phys. Chem. C XXXX, XXX, XXX−XXX

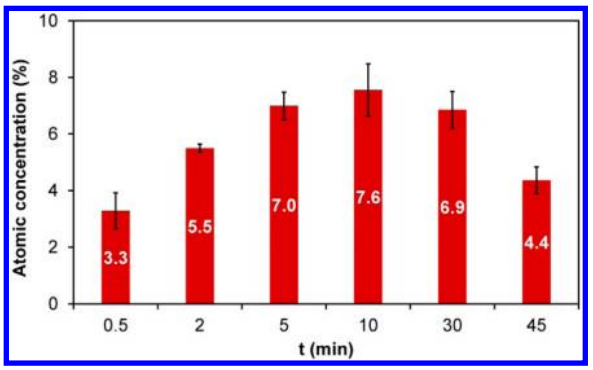

Figure 3. Influence of exposure time on the XPS chlorine atomic concentration.

treatment times. Thus, it is expected that, when the plasma interact with the carbon atoms, chlorine species can be attached to them or can break bonds.

The first process results in an increase in functionalization that seems to be prevalent up to 10 min of treatment. The second one seems to be important at longer times and results in the partial etching of the surface atoms of the MWCNTs and in a lower degree of functionalization. In fact, it is known that plasma microwave devices are frequently used to eliminate the carbon contents of mineral coals by gasification at low temperature without altering the mineral residues, which is usually achieved after long treatments.

The high-resolution (C 1s and Cl 2p) XPS spectra of the sample obtained after treatment with plasma for 10 min are collected in Figure 4 (see Figures S-1 and S-2 in the Supporting Information for the high-resolution spectra of the O 1s and N 1s peaks of samples treated at different times). The C 1s spectrum of the original sample was intrinsically asymmetric, and the chemical changes produced by the plasma treatment resulted in an increase in asymmetry of the peak because of the

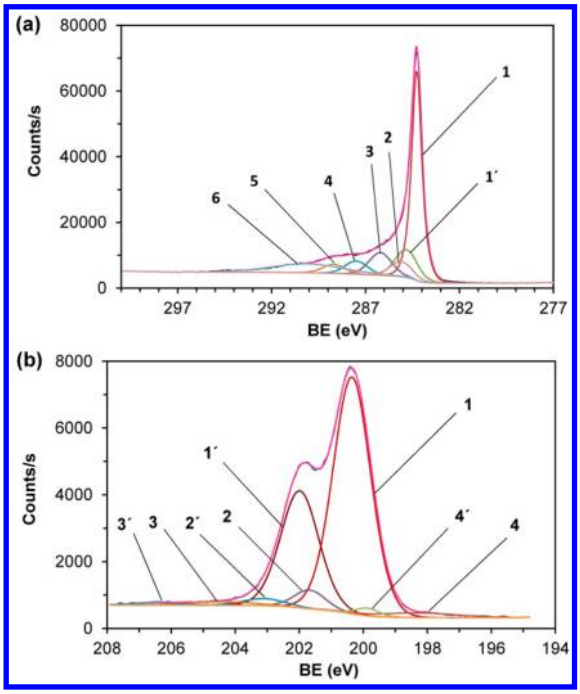

Figure 4. Deconvolution of high-resolution XPS spectra of the sample treated for 10 min: (a) C 1s peak and (b) Cl 2p peak.

introduced chlorine chemical functionalities. Chlorine has significant effects on the electronic screening of the carbon atoms to which it is bound, because of its electronegativity. Thus, the shift of the C 1s peak to lower binding energies has been reported.[36,39,53,54] Dettlaf-Weglikowska et al.[36,39] explained this behavior as an effect of the electron-accepting character of the chlorine attached to the surface of the nanotubes. Nevertheless, in our case, no shift of the C 1s peak was observed but only an increase in the peak asymmetry. Similarly, Hanelt et al.[31] reported asymmetric graphitic and three additional components on the C 1s peak of carbon nanotubes functionalized with bromine. Barthos et al.[55] also reported the deconvolution of the C 1s peak of chlorine carbon nanotubes in which they include only one C—Cl component at 287.7 eV. Nevertheless it has also been reported that the carbon atoms that are not directly bond to chlorine but are neighbors of C—Cl functions are affected by an inductive effect.[56,57] Thus, the deconvolution of the C 1s peak can result in several components.[58−61] As shown in Figure 4a, we have deconvoluted the C 1s peak into several components as suggested by Papirer et al.,[60] who considered several chemical environments (the following order numbers coincide with those appended to the components in Figure 4a):

(1) graphitic and nonconjugated carbon that appear at 284.3 eV (number 1) and 284.8 eV (number 1′), respectively;
(2) chlorine bonded to sp^2 carbon atoms (C_{sp^2}—Cl) in the outer border of polyaromatic structures at 285.3 eV;
(3) chlorine bonded to one sp^3 carbon (C_{sp^3}—Cl) or to two sp^2 carbons (C_{sp^2}—Cl—C_{sp^2}) at 286.4 eV;
(4) two chlorine atoms bonded to sp^3 carbon (C_{sp^3}—Cl_2) at 287.3 eV;
(5) the component at 288.6 eV assigned to two chlorine atoms bonded to an sp^3 carbon that is also bonded to a C—Cl group (Cl_2—C_{sp^3}—C—Cl); and
(6) the shakeup satellite component appearing at 289.7 eV, which might also be due to three chlorine atoms bonded to a carbon atom that it is also bonded to an sp^2 carbon, namely, Cl_3—C—C_{sp^2} groups.

Thus, the XPS data seem to suggest that chlorine is covalently bound in up to five different chemical environments. This conclusion is related to two factors: the different carbon atoms in MWCNTs and the several species resulting from the cold plasma. Thus, the carbon atoms can be sp^2 or sp^3 (the latter are at the borders and vacancies of the tubes), and the plasma chlorine species can be $Cl^{\bullet}$, $ClC^{\bullet}$, $ClC_2^{\bullet}$, and $ClC_3^{\bullet}$. It has to be considered that the component at 285.3 eV (2 in Figure 4a) can also be assigned to C—N═C (sp^2) groups and that at 286.4 eV (3 in Figure 4a) might also be due to C—O or —C—N (sp^3) groups. In addition, the components at 287.3 eV (4 in Figure 5a) and 288.6 eV (5 in Figure 4a) can also be assigned to carbonyls and carboxyls, respectively.[61−63] The high-resolution Cl 2p peak (Figure 4b) shows the $^1/_2$ (labeled 1−4) and $^3/_2$ (1′−4′) components due to spin−orbit coupling. The deconvolution of the peaks results in a mean component at 200.4 eV due to Cl—C (sp^2 or sp^3) groups. The component at 201.7 eV (2 in Figure 4b) is assigned to Cl_3—C—C (sp^2) groups in the outer border of the nanotubes. There are also two smaller components at 204.4 and 198.4 eV (3 and 4 in Figure 4b), which might be due to occluded chlorine and chloride, respectively.[60] Evidence of the C—Cl bond can also be found in the FTIR spectra of the treated samples,[32,38] which show a band at 750 cm^{-1} (see Figure S-3, Supporting Information).

dx.doi.org/10.1021/jp404390h | J. Phys. Chem. C XXXX, XXX, XXX−XXX

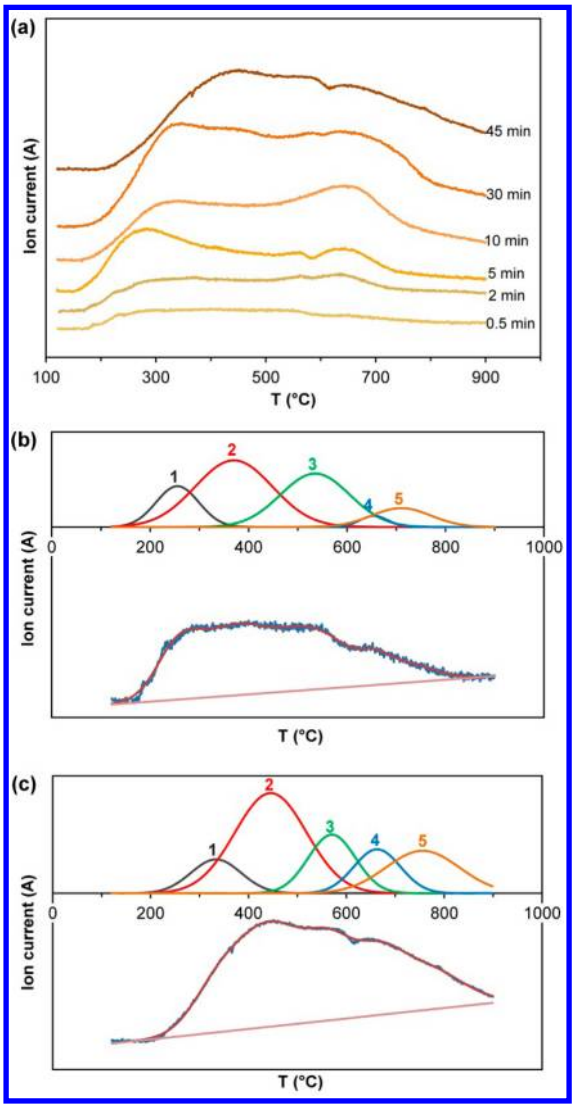

Figure 5. (a) TPD profiles of HCl desorbed from samples obtained after different exposure times (from 0.5 to 45 min). (b,c) Deconvolutions of the HCl desorbed profiles of the samples treated for (b) 0.5 and (c) 45 min.

The thermal stability of the chlorine groups can be seen in the TPD profiles in Figure 5. It is worth mentioning that 36 (HCl) was the main desorbed mass detected by the spectrometer, although other masses related to chlorine (atomic chlorine and molecular chlorine) were also detected. The HCl evolution was larger for samples obtained after longer periods of plasma treatment. In addition, it was seen that the evolution occurred over a wide range of temperature.

This means that the covalent attachment of chlorine results in a multimodal distribution of chemical groups over a wide range of stability. Similar behavior was reported[9] in fluorinated single-walled carbon nanotubes, showing that covalently bonded fluorine still remained after the samples had been heated at 550 °C. The shoulder at low temperature (near 260 °C), which is not clearly distinguished in samples treated for 0.5 and 2 min, was found to increase and shift to higher temperatures at long treatments. As already commented, this is probably because the gasification of the nanotubes partially removes the less stable chlorine groups.

As the high-resolution XPS spectra suggest up to five chlorine chemical environments, the TPD profiles were also deconvoluted, as an approximation, into five components using Gaussian curves. The deconvolutions, such as those of the samples obtained after 0.5 and 45 min of treatment (Figure 5b,c), resulted in good fittings to the experimental data (r^2 = 0.989 and 0.999, respectively).

Figure 6 shows how the temperatures of the maxima of the deconvoluted desorption peaks vary with the time of treatment.

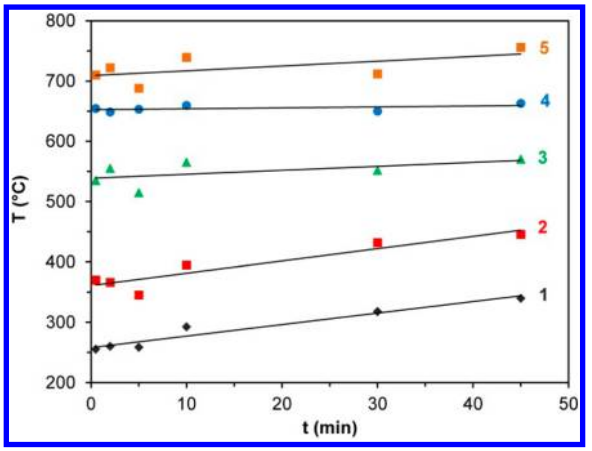

Figure 6. Variation of the desorption temperature of different chlorine groups with the time of treatment.

These data can provide some information on how the stabilities of the different chemical environments change during plasma treatment. This figure suggests that the time of plasma treatment tends to shift the maxima to higher temperatures, in particular those of relatively low temperatures (1 and 2). Again, this behavior can be related to the partial etching of the MWCNTs, in agreement with the earlier statements. Indeed, the chemical groups that more easily evolve are less stable, so longer plasma treatments allow for their elimination. As a consequence, longer treatment times result in an increase in the stability of the chlorine groups. The stabilities of the chlorine groups evolving at around 550 and 650 °C were found to be almost unchanged with the time of treatment.

An important aspect of covalent functionalization is related to the sites where chlorine is attached and whether this process changes the textural characteristics of the MWCNTs. The former issue can be considered by analyzing several components of the high-resolution core-level C 1s XPS spectra (Figure 4a), whereas the effect on the textural characteristics can be determined from nitrogen adsorption isotherms and X-ray diffractograms. Figure 7 displays the variation of some components of the C 1s XPS peak, specifically the percentages of graphitic, nonconjugated carbon, and shakeup satellite components, as a function of the chlorine content. The graphitic carbon percentage decreased as a consequence of the covalent attachment of chlorine. Nevertheless, this grafting was not produced on the nanotubes walls, as can be deduced from the almost constant value of the shakeup component, which is related to the conjugation of the aromatic arene centers of the nanotube walls. Thus, the attachment of the chlorine atoms to the wall sp^2 carbons must be related to the decrease in this component. Therefore, the plasma treatment mainly attaches chlorine to borders, defects, or irregularities of the carbon nanotubes. The decrease of the nonconjugated carbon

dx.doi.org/10.1021/jp404390h | J. Phys. Chem. C XXXX, XXX, XXX–XXX

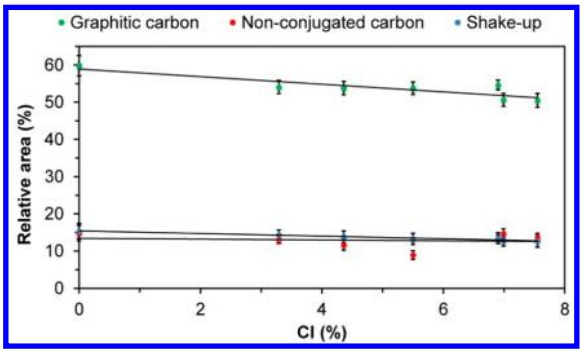

Figure 7. Variation of the relative amounts of three different types of C atoms with the degree of chlorination of the samples.

component points to a partial gasification of amorphous carbon during the treatment.

It is known that halogens tend to form intercalation compounds with graphite. These compounds have larger interlayer spacing than the parent graphite. We used X-ray diffraction to analyze whether the chlorine was, in part, in the interlayer graphene space of the multiwalled nanotubes. The diffractograms of the samples did not show any change in the value of the 2θ angle (Figure S-4, Supporting Information). Thus, the original MWCNTs had an interlayer spacing of 0.347 nm, which is almost the same as those for samples treated with plasma (between 0.348 and 0.347 nm for samples obtained after 0.5, 10, and 45 min of treatment), which suggests that no chlorine intercalation resulted from the treatment.

The effect of the plasma treatment on the textural characteristics of the samples was also analyzed by nitrogen adsorption at 77 K. The adsorption isotherms of all samples were found to be of type II, characteristic of nonporous materials, and superimposable (Figure S-5, Supporting Information). Therefore, almost no textural modification of the carbon nanotubes was produced by the plasma treatment. This is also reflected in the Brunauer–Emmett–Teller (BET) surface areas, which range from 240 $m^2\ g^{-1}$ for the original sample to 211 and 249 $m^2\ g^{-1}$ for the samples obtained after 2 and 45 min, respectively, of plasma treatment. Similarly, the micropore volumes obtained by applying the Dubinin–Radushkevich equation to the adsorption data at very low pressures (indicating the presence of a scarce microporosity) range from 0.091 $cm^3\ g^{-1}$ for the original MWCNTs to 0.080 and 0.094 $cm^3\ g^{-1}$ for the same samples, clearly showing that the variation in the textural characteristics can be considered negligible.

We also attempted to gain insight into the thermal characteristics of the oxygen functionalities, as oxygen attachment (Table 1) is a side effect of our CCl_4 plasma treatment. Thus, the thermal stability of the oxygen-containing groups can be seen in the selected TPD profiles of Figure 8. The samples were found to desorb carbon dioxide in a wide range of temperatures (between 200 and 800 °C). The samples obtained after 0.5 and 5 min of treatment had two maxima, near 600 and 700 °C, and the sample obtained after 10 min also had a maximum near 225 °C. The carbon dioxide desorbed at lower temperatures is due to carboxylic groups, and that desorbed at high temperatures is usually assigned to lactones and anhydrides. Thus, the oxygen groups resulting from the plasma treatments had several chemical natures and a wide range of stabilization energies, but none of them evolved at temperatures of less than 200 °C. This suggests that this oxygen

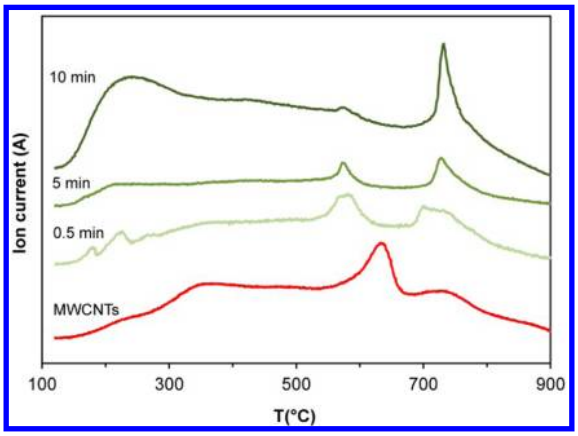

Figure 8. TPD profiles of CO_2 desorbed from pristine MWCNTs and samples obtained after three different exposure times.

is not physically adsorbed but rather covalently bonded (chemisorbed), which points to an origin probably related to the residual air in the plasma chamber device.

The carbon monoxide desorption was almost negligible. Only the sample treated for 10 min had a band with a maximum near 225 °C and also low desorption at temperatures higher than 600 °C. The first peak near 225 °C is coincident with that of the CO_2 profile. It is probably the result of the condensation of several adjacent oxygen-containing groups,[64−66] or it could also be partially generated by the fragmentation of CO_2.

The O 1s spectra (Figure S-1, Supporting Information) have three components at ∼531, 533, and 535 eV. The first of these is usually assigned to O═C groups in single- and multiwalled carbon nanotubes, carbon fibers, and activated carbons that have been oxidized with several oxidants (including nitric acid), whereas the second is usually assigned to O—C.[59,67−71] The assignment of the component at ∼535 eV is a matter of controversy, with some authors assigning it to O—H groups[67,70] and others assigning it to carboxyls.[69]

The N 1s spectrum has two components at ∼399 and 401 eV. The former is usually asigned to N—H groups, whereas the second is closer to 400.9 eV, which is usually assigned to N bonded to C, than to 406.7 eV, which is assigned to N—O groups.[59]

CONCLUSIONS

An efficient, fast, clean, and reliable method for the chlorination of MWCNTs using microwave cold plasma has been established. The efficiency of the procedure is improved if the nanotubes are pretreated with helium plasma, reaching much higher degrees of chlorine functionalization than those previously reported. The chlorine is covalently bonded to the carbon surface in up to five different chemical environments, which are mainly located in borders or defects of the tubes, so that the walls of the nanotubes remain mostly unchanged, preserving the conjugation in the sp^2 graphene sheets. Moreover, no intercalation of chlorine between the graphene sheets is produced, and the textural characteristics are not modified, maintaining the tube properties. The high concentration of chlorine surface atoms achieved, together with the capacity of the chlorine atoms to act as leaving groups in many organic reactions, make the proposed method a very interesting and promising first step for further selective functionalization of carbon nanotubes with complex molecules, widening the range

dx.doi.org/10.1021/jp404390h | J. Phys. Chem. C XXXX, XXX, XXX−XXX

of potential applications. This methodology can also be extrapolated to the functionalization of other forms of carbon materials.

■ ASSOCIATED CONTENT

Supporting Information

High-resolution spectra of O 1s and N 1s XPS peaks, FTIR spectra, XRD diffraction diagrams, and N_2 adsorption isotherms of some treated samples. This material is available free of charge via the Internet at http://pubs.acs.org.

■ AUTHOR INFORMATION

Corresponding Author

*E-mail: mjperezm@ugr.es.

Notes

The authors declare no competing financial interest.

■ ACKNOWLEDGMENTS

The support of the Ministerio de Economía y Competitividad (Projects MAT2009-14185-C02-01 and MAT2009-14185-C02-02) and the Autonomous Regional Government (J. de Andalucia, Proyecto de Excelencia ref P09-FQM-4765 and grupos RNM342 and FQM273) is acknowledged. V.K.A. also acknowledges a Ph.D. fellowship from the FPI Program (Ministerio de Economía y Competitividad).

■ REFERENCES

(1) Krueger, A. *Carbon Materials and Nanotechnology*; Wiley-VCH Verlag GmbH & Co. KGaA: Weinheim, Germany, 2010.
(2) Peng, X. H.; Wong, S. S. Functional Covalent Chemistry of Carbon Nanotube Surfaces. *Adv. Mater.* **2009**, *21*, 625−642.
(3) Balasubramanian, K.; Burghard, M. Chemically Functionalized Carbon Nanotubes. *Small* **2005**, *1*, 180−192.
(4) Spitalsky, Z.; Tasis, D.; Papagelis, K.; Galiotis, C. Carbon Nanotube−Polymer Composites: Chemistry, Processing, Mechanical and Electrical Properties. *Prog. Polym. Sci.* **2010**, *35*, 357−401.
(5) Tasis, D.; Tagmatarchis, N.; Bianco, A.; Prato, M. Chemistry of Carbon Nanotubes. *Chem. Rev.* **2006**, *106*, 1105−1136.
(6) Bose, S.; Khare, R. A.; Moldenaers, P. Assessing the Strengths and Weaknesses of Various Types of Pre-Treatments of Carbon Nanotubes on the Properties of Polymer/Carbon Nanotubes Composites: A Critical Review. *Polymer* **2010**, *51*, 975−993.
(7) Gonzalez-Dominguez, J. M.; Gonzalez, M.; Anson-Casaos, A.; Diez-Pascual, A. M.; Gomez, M. A.; Martinez, M. T. Effect of Various Aminated Single-Walled Carbon Nanotubes on the Epoxy Cross-Linking Reactions. *J. Phys. Chem. C* **2011**, *115*, 7238−7248.
(8) Lehman, J. H.; Terrones, M.; Mansfield, E.; Hurst, K. E.; Meunier, V. Evaluating the Characteristics of Multiwall Carbon Nanotubes. *Carbon* **2011**, *49*, 2581−2602.
(9) Alemany, L. B.; Zhang, L.; Zeng, L.; Edwards, C. L.; Barron, A. R. Solid-State NMR Analysis of Fluorinated Single-Walled Carbon Nanotubes: Assessing the Extent of Fluorination. *Chem. Mater.* **2007**, *19*, 735−744.
(10) Zeng, L.; Alemany, L. B.; Edwards, C. L.; Barron, A. R. Demonstration of Covalent Sidewall Functionalization of Single Wall Carbon Nanotubes by NMR Spectroscopy: Side Chain Length Dependence on the Observation of the Sidewall sp^3 Carbons. *Nano Res.* **2008**, *1*, 72−88.
(11) Singh, P.; Campidelli, S.; Giordani, S.; Bonifazi, D.; Bianco, A.; Prato, M. Organic Functionalisation and Characterisation of Single-Walled Carbon Nanotubes. *Chem. Soc. Rev.* **2009**, *38*, 2214−2230.
(12) Hirsch, A.; Vostrowsky, O. Functionalization of Carbon Nanotubes. In *Functional Molecular Nanostructures*; Schluter, A. D., Ed.; Springer: Berlin, 2005; Vol. *245*, pp 193−237.
(13) Dillon, E. P.; Crouse, C. A.; Barron, A. R. Synthesis, Characterization, and Carbon Dioxide Adsorption of Covalently Attached Polyethyleneimine-Functionalized Single-Wall Carbon Nanotubes. *ACS Nano* **2008**, *2*, 156−164.
(14) Hirsch, A. Functionalization of Single-Walled Carbon Nanotubes. *Angew. Chem., Int. Ed.* **2002**, *41*, 1853−1859.
(15) Wepasnick, K. A.; Smith, B. A.; Schrote, K. E.; Wilson, H. K.; Diegelmann, S. R.; Fairbrother, D. H. Surface and Structural Characterization of Multi-Walled Carbon Nanotubes Following Different Oxidative Treatments. *Carbon* **2011**, *49*, 24−36.
(16) Zschoerper, N. P.; Katzenmaier, V.; Vohrer, U.; Haupt, M.; Oehr, C.; Hirth, T. Analytical Investigation of the Composition of Plasma-Induced Functional Groups on Carbon Nanotube Sheets. *Carbon* **2009**, *47*, 2174−2185.
(17) Yang, D.-Q.; Sacher, E. Strongly Enhanced Interaction between Evaporated Pt Nanoparticles and Functionalized Multiwalled Carbon Nanotubes via Plasma Surface Modifications: Effects of Physical and Chemical Defects. *J. Phys. Chem. C* **2008**, *112*, 4075−4082.
(18) Simmons, J. M.; Nichols, B. M.; Baker, S. E.; Marcus, M. S.; Castellini, O. M.; Lee, C. S.; Hamers, R. J.; Eriksson, M. A. Effect of Ozone Oxidation on Single-Walled Carbon Nanotubes. *J. Phys. Chem. B* **2006**, *110*, 7113−7118.
(19) Mawhinney, D. B.; Naumenko, V.; Kuznetsova, A.; Yates, J. T.; Liu, J.; Smalley, R. E. Infrared Spectral Evidence for the Etching of Carbon Nanotubes: Ozone Oxidation at 298 K. *J. Am. Chem. Soc.* **2000**, *122*, 2383−2384.
(20) Cai, L. T.; Bahr, J. L.; Yao, Y. X.; Tour, J. M. Ozonation of Single-Walled Carbon Nanotubes and Their Assemblies on Rigid Self-Assembled Monolayers. *Chem. Mater.* **2002**, *14*, 4235−4241.
(21) Byl, O.; Liu, J.; Yates, J. T. Etching of Carbon Nanotubes by Ozone—A Surface Area Study. *Langmuir* **2005**, *21*, 4200−4204.
(22) Banerjee, S.; Wong, S. S. Rational Sidewall Functionalization and Purification of Single-Walled Carbon Nanotubes by Solution-Phase Ozonolysis. *J. Phys. Chem. B* **2002**, *106*, 12144−12151.
(23) Hemraj-Benny, T.; Bandosz, T. J.; Wong, S. S. Effect of Ozonolysis on the Pore Structure, Surface Chemistry, and Bundling of Single-Walled Carbon Nanotubes. *J. Colloid Interface Sci.* **2008**, *317*, 375−382.
(24) Peng, K.; Liu, L.-Q.; Li, H.; Meyer, H.; Zhang, Z. Room Temperature Functionalization of Carbon Nanotubes Using an Ozone/Water Vapor Mixture. *Carbon* **2011**, *49*, 70−76.
(25) Chen, Z. Y.; Ziegler, K. J.; Shaver, J.; Hauge, R. H.; Smalley, R. E. Cutting of Single-Walled Carbon Nanotubes by Ozonolysis. *J. Phys. Chem. B* **2006**, *110*, 11624−11627.
(26) Bittencourt, C.; Van Lier, G.; Ke, X.; Suarez-Martinez, I.; Felten, A.; Ghijsen, J.; Van Tendeloo, G.; Ewels, C. P. Spectroscopy and Defect Identification for Fluorinated Carbon Nanotubes. *ChemPhysChem* **2009**, *10*, 920−925.
(27) Wang, Y. Q.; Sherwood, P. M. A. Studies of Carbon Nanotubes and Fluorinated Nanotubes by X-ray and Ultraviolet Photoelectron Spectroscopy. *Chem. Mater.* **2004**, *16*, 5427−5436.
(28) Bulusheva, L. G.; Fedoseeva, Y. V.; Okotrub, A. V.; Flahaut, E.; Asanov, I. P.; Koroteev, V. O.; Yaya, A.; Ewels, C. P.; Chuvilin, A. L.; Felten, A.; Van Lier, G.; Vyalikh, D. V. Stability of Fluorinated Double-Walled Carbon Nanotubes Produced by Different Fluorination Techniques. *Chem. Mater.* **2010**, *22*, 4197−4203.
(29) Peng, H. Q.; Gu, Z. N.; Yang, J. P.; Zimmerman, J. L.; Willis, P. A.; Bronikowski, M. J.; Smalley, R. E.; Hauge, R. H.; Margrave, J. L. Fluorotubes as Cathodes in Lithium Electrochemical Cells. *Nano Lett.* **2001**, *1*, 625−629.
(30) Friedrich, J. F.; Wettmarshausen, S.; Hanelt, S.; Mach, R.; Mix, R.; Zeynalov, E. B.; Meyer-Plath, A. Plasma-Chemical Bromination of Graphitic Materials and Its Use for Subsequent Functionalization and Grafting of Organic Molecules. *Carbon* **2010**, *48*, 3884−3894.
(31) Hanelt, S.; Friedrich, J. F.; Orts-Gil, G.; Meyer-Plath, A. Study of Lewis Acid Catalyzed Chemical Bromination and Bromoalkylation of Multi-Walled Carbon Nanotubes. *Carbon* **2012**, *50*, 1373−1385.
(32) Unger, E.; Graham, A.; Kreupl, F.; Liebau, M.; Hoenlein, W. Electrochemical Functionalization of Multi-Walled Carbon Nanotubes for Solvation and Purification. *Curr. Appl. Phys.* **2002**, *2*, 107−111.

(33) Fagan, S. B.; da Silva, A. J. R.; Mota, R.; Baierle, R. J.; Fazzio, A. Functionalization of Carbon Nanotubes through the Chemical Binding of Atoms and Molecules. *Phys. Rev. B* **2003**, *67*, 033405-1−033405-4.
(34) Kónya, Z.; Vesselenyi, I.; Niesz, K.; Kukovecz, A.; Demortier, A.; Fonseca, A.; Delhalle, J.; Mekhalif, Z.; Nagy, J. B.; Koós, A. A.; Osváth, Z.; Kocsonya, A.; Biró, L. P.; Kiricsi, I. Large Scale Production of Short Functionalized Carbon Nanotubes. *Chem. Phys. Lett.* **2002**, *360*, 429−435.
(35) Lee, W. H.; Kim, S. J.; Lee, W. J.; Lee, J. G.; Haddon, R. C.; Reucroft, P. J. X-ray Photoelectron Spectroscopic Studies of Surface Modified Single-Walled Carbon Nanotube Material. *Appl. Surf. Sci.* **2001**, *181*, 121−127.
(36) Dettlaff-Weglikowska, U.; Skákalová, V.; Graupner, R.; Jhang, S. H.; Kim, B. H.; Lee, H. J.; Ley, L.; Park, Y. W.; Berber, S.; Tománek, D.; Roth, S. Effect of $SOCl_2$ Treatment on Electrical and Mechanical Properties of Single-Wall Carbon Nanotube Networks. *J. Am. Chem. Soc.* **2005**, *127*, 5125−5131.
(37) Lockett, M. R.; Smith, L. M. Attaching Molecules to Chlorinated and Brominated Amorphous Carbon Substrates via Grignard Reactions. *Langmuir* **2009**, *25*, 3340−3343.
(38) Wang, D.-W.; Wu, K.-H.; Gentle, I. R.; Lu, G. Q. Anodic Chlorine/Nitrogen Co-Doping of Reduced Graphene Oxide Films at Room Temperature. *Carbon* **2012**, *50*, 3333−3341.
(39) Dettlaff-Weglikowska, U.; Benoit, J. M.; Chiu, P. W.; Graupner, R.; Lebedkin, S.; Roth, S. Chemical Functionalization of Single Walled Carbon Nanotubes. *Curr. Appl. Phys.* **2002**, *2*, 497−501.
(40) Baytekin, H. T.; Wirth, T.; Gross, T.; Treu, D.; Sahre, M.; Theisen, J.; Schmidt, M.; Unger, W. E. S. Determination of Wettability of Surface-Modified Hot-Embossed Polycarbonate Wafers Used in Microfluidic Device Fabrication via XPS and ToF-SIMS. *Surf. Interface Anal.* **2008**, *40*, 358−363.
(41) Bubert, H.; Haiber, S.; Brandl, W.; Marginean, G.; Heintze, M.; Bruser, V. Characterization of the Uppermost Layer of Plasma-Treated Carbon Nanotubes. *Diamond Relat. Mater.* **2003**, *12*, 811−815.
(42) Bulusheva, L. G.; Okotrub, A. V.; Flahaut, E.; Asanov, I. P.; Gevko, P. N.; Koroteev, V. O.; Fedoseeva, Y. V.; Yaya, A.; Ewels, C. P. Bromination of Double-Walled Carbon Nanotubes. *Chem. Mater.* **2012**, *24*, 2708−2715.
(43) Colomer, J. F.; Marega, R.; Traboulsi, H.; Meneghetti, M.; Van Tendeloo, G.; Bonifazi, D. Microwave-Assisted Bromination of Double-Walled Carbon Nanotubes. *Chem. Mater.* **2009**, *21*, 4747−4749.
(44) Felten, A.; Bittencourt, C.; Pireaux, J. J.; Van Lier, G.; Charlier, J. C. Radio-Frequency Plasma Functionalization of Carbon Nanotubes Surface O_2, NH_3, and CF_4 Treatments. *J. Appl. Phys.* **2005**, *98*.
(45) Felten, A.; Ghijsen, J.; Pireaux, J. J.; Johnson, R. L.; Whelan, C. M.; Liang, D.; Van Tendeloo, G.; Bittencourt, C. Photoemission Study of CF_4 rf-Plasma Treated Multi-Wall Carbon Nanotubes. *Carbon* **2008**, *46*, 1271−1275.
(46) Grimblot, J.; Mutel, B.; Moineau, V.; Colson, T.; Dessaux, O.; Goudmand, P. Comparative Study by XPS of Nitrogen and Oxygen Implantation in Different Carbonaceous Polymers Using Flowing Nitrogen Plasma. *Surf. Interface Anal.* **2000**, *30*, 415−419.
(47) Khare, B.; Wilhite, P.; Tran, B.; Teixeira, E.; Fresquez, K.; Mvondo, D. N.; Bauschlicher, C.; Meyyappan, M. Functionalization of Carbon Nanotubes via Nitrogen Glow Discharge. *J. Phys. Chem. B* **2005**, *109*, 23466−23472.
(48) Vohrer, U.; Zschoerper, N. P.; Koehne, Y.; Langowski, S.; Oehr, C. Plasma Modification of Carbon Nanotubes and Bucky Papers. *Plasma Processes Polym.* **2007**, *4*, S871−S877.
(49) Yan, Y. H.; Cui, J.; Chan-Park, M. B.; Wang, X.; Wu, Q. Y. Systematic Studies of Covalent Functionalization of Carbon Nanotubes via Argon Plasma-Assisted UV Grafting. *Nanotechnology* **2007**, *18*.
(50) Harry, J. E. *Introduction to Plasma Technology*; Wiley-VCH: Weinheim, Germany, 2010.
(51) Domingo-Garcia, M.; Lopez-Garzon, F. J.; Perez-Mendoza, M. Modifications Produced by O_2 Plasma Treatments on a Mesoporous Glassy Carbon. *Carbon* **2000**, *38*, 555−563.
(52) Lopez-Garzon, F. J.; Domingo-Garcia, M.; Perez-Mendoza, M.; Alvarez, P. M.; Gomez-Serrano, V. Textural and Chemical Surface Modifications Produced by Some Oxidation Treatments of a Glassy Carbon. *Langmuir* **2003**, *19*, 2838−2844.
(53) Qian, Z.; Ma, J.; Zhou, J.; Lin, P.; Chen, C.; Chen, J.; Feng, H. Facile Synthesis of Halogenated Multi-Walled Carbon Nanotubes and Their Unusual Photoluminescence. *J. Mater. Chem.* **2012**, *22*, 22113−22119.
(54) Rafailov, P. M.; Thomsen, C.; Monev, M.; Dettlaff-Weglikowska, U.; Roth, S. Electrochemical Functionalization of SWNT Bundles in Acid and Salt Media as Observed by Raman and X-ray Photoelectron Spectroscopy. *Phys. Status Solidi B* **2008**, *245*, 1967−1970.
(55) Barthos, R.; Mehn, D.; Demortier, A.; Pierard, N.; Morciaux, Y.; Demortier, G.; Fonseca, A.; Nagy, J. B. Functionalization of Single-Walled Carbon Nanotubes by Using Alkyl-Halides. *Carbon* **2005**, *43*, 321−325.
(56) Köver, L. Chemical Effects in XPS. In *Surface Analysis by Auger and X-ray Photoelectron Spectroscopy*; Briggs, D., Grant, J. T., Eds.; IM Publications: Chichester, U.K., 2003; Chapter 16.
(57) Watts, J. F.; Wolstenholme, J. *An Introduction to Surface Analisys by Electron Microscopy*; John Wiley & Sons Inc: Chichester, U.K., 2003; pp 1−200.
(58) Bittencourt, C.; Navio, C.; Nicolay, A.; Ruelle, B.; Godfroid, T.; Snyders, R.; Colomer, J. F.; Lagos, M. J.; Ke, X.; Van Tendeloo, G.; Suarez-Martinez, I.; Ewels, C. P. Atomic Oxygen Functionalization of Vertically Aligned Carbon Nanotubes. *J. Phys. Chem. C* **2011**, *115*, 20412−20418.
(59) Kundu, S.; Wang, Y.; Xia, W.; Muhler, M. Thermal Stability and Reducibility of Oxygen-Containing Functional Groups on Multiwalled Carbon Nanotube Surfaces: A Quantitative High-Resolution XPS and TPD/TPR Study. *J. Phys. Chem. C* **2008**, *112*, 16869−16878.
(60) Papirer, E.; Lacroix, R.; Donnet, J. B.; Nanse, G.; Fioux, P. XPS Study of the Halogenation of Carbon Black—Part 2. Chlorination. *Carbon* **1995**, *33*, 63−72.
(61) Morant, C.; Andrey, J.; Prieto, P.; Mendiola, D.; Sanz, J. M.; Elizalde, E. XPS Characterization of Nitrogen-Doped Carbon Nanotubes. *Phys. Status Solidi A* **2006**, *203*, 1069−1075.
(62) Gromov, A. V.; Gray, N.; Szilagyi, P. A.; Campbell, E. E. B. Direct Grafting of Carbon Nanotubes with Ethylenediamine. *J. Mater. Chem.* **2012**, *22*, 21242−21248.
(63) Peñas-Sanjuan, A.; Lopez-Garzon, R.; Domingo-Garcia, M.; Javier Lopez-Garzon, F.; Melguizo, M.; Perez-Mendoza, M. An Efficient Procedure to Bond Nanostructured Nitrogen Functionalities to Carbon Surfaces. *Carbon* **2012**, *50*, 3977−3986.
(64) Domingo-Garcia, M.; Groszek, A. J.; Lopez-Garzon, F. J.; Perez-Mendoza, M. Dynamic Adsorption of Ammonia on Activated Carbons Measured by Flow Microcalorimetry. *Appl. Catal. A: Gen.* **2002**, *233*, 141−150.
(65) Perez-Mendoza, M.; Domingo-Garcia, M.; Lopez-Garzon, F. J. Carbon Materials as Catalysts for Methylamines Synthesis. *Appl. Catal. A: Gen.* **2002**, *224*, 239−253.
(66) Domingo-Garcia, M.; Garzon, F. J. L.; Perez-Mendoza, M. J. On the Characterization of Chemical Surface Groups of Carbon Materials. *J. Colloid Interface Sci.* **2002**, *248*, 116−122.
(67) Biniak, S.; Szymanski, G.; Siedlewski, J.; Swiatkowski, A. The Characterization of Activated Carbons with Oxygen and Nitrogen Surface Groups. *Carbon* **1997**, *35*, 1799−1810.
(68) Chiang, Y.-C.; Lin, W.-H.; Chang, Y.-C. The Influence of Treatment Duration on Multi-Walled Carbon Nanotubes Functionalized by H_2SO_4/HNO_3 Oxidation. *Appl. Surf. Sci.* **2011**, *257*, 2401−2410.
(69) Lakshminarayanan, P. V.; Toghiani, H.; Pittman, C. U. Nitric Acid Oxidation of Vapor Grown Carbon Nanofibers. *Carbon* **2004**, *42*, 2433−2442.
(70) Martínez, M. T.; Callejas, M. A.; Benito, A. M.; Cochet, M.; Seeger, T.; Ansón, A.; Schreiber, J.; Gordon, C.; Marhic, C.; Chauvet, O.; Fierro, J. L. G.; Maser, W. K. Sensitivity of Single Wall Carbon

Nanotubes to Oxidative Processing: Structural Modification, Intercalation and Functionalisation. *Carbon* **2003**, *41*, 2247−2256.
(71) Zielke, U.; Huttinger, K. J.; Hoffman, W. P. Surface-Oxidized Carbon Fibers. 1. Surface Structure and Chemistry. *Carbon* **1996**, *34*, 983−998.